Check for updates

Thermal conductivity and balanced performance in infrared nonlinear optical multicomponent chalcogenides $Li_xAg_{1-x}Ga_yIn_{1-y}Se_2$†

L. I. Isaenko,*[a,c] Bohui Xu, [iD][b,d] K. E. Korzhneva,[a] Pifu Gong, [iD][b] D. A. Samoshkin,[e] A. F. Kurus [iD][a,c] and Zheshuai Lin [iD] *[b,d]

The performance of infrared (IR) nonlinear optical (NLO) materials is significantly affected by the thermal conductivity k_L, but studies on the structure and property relationship of k_L in these materials are very rare. In this work we evaluated the k_L in IR NLO multicomponent chalcogenides $Li_xAg_{1-x}Ga_yIn_{1-y}Se_2$ with a smooth change in the compositions x and y by using a machine learning approach and laser flash measurements, combined with available experimental results. The found patterns of k_L dependence on the atomic mass, bond length and electronegativity provide an effective understanding for navigation in the process of searching for new chalcogenide crystals with an optimal set of parameters that allow them to be effectively used as a frequency converter of laser radiation in the IR range. Moreover, the compositions $Li_{0.5}Ag_{0.5}GaSe_2$, $Li_{0.81}Ag_{0.19}InSe_2$ and $AgGa_{0.5}In_{0.5}Se_2$ are demonstrated to exhibit a balanced combination of the parameters k_L, NLO effects, energy band gaps, and birefringence for IR NLO applications.

Introduction

It is well known that infrared (IR) spectroscopy measurements, *e.g.*, the IR transmission spectrum, reflect vibrational modes unique to the molecules in the sample, and are thereby widely used to characterize the vast majority of chemical compounds. On this basis, highly sensitive compact high-resolution laser spectrometers are being developed to solve analytical and scientific problems, including studies of ultra-fast processes in a wide spectral range of up to 18 μm and even the THZ region.[1,2] An efficient assignment of such widely tunable systems is provided by lasers produced from the frequency conversion using IR nonlinear optical (NLO) crystals, which should meet an optimal combination of performance, including a high nonlinear second harmonic generation (SHG) coefficient d_{ij} comparable to that in $AgGaS_2$ (with d_{36} = 13.40 pm V^{-1}), a wide range of transparency, moderate birefringence Δn = 0.03–0.10 to achieve the phase matching condition, as well

as a large band gap E_g preferably >3.00 eV for optical stability, *etc.*[3–7] In the past decades, quite a few IR NLO crystals have been developed in the chalcogenides in the ABC_2 family (A = Ag, Li; B = Ga, In; and C = S, Se), which exhibits a wide IR transparent window and a relatively strong SHG effect.[8–12]

It should be emphasized that balancing all the necessary performance is a big issue in the discovery of IR NLO crystals because these requirements are often contradictory. For example, an increase in the band gap will lead to a decrease in the SHG coefficient.[13] On the other hand, the laser-induced damage threshold (LIDT) for a crystal (independent of the presence of impurities and defects) can be increased by increasing the band gap E_g, because it can effectively suppress the occurrence of two- or multi-photon absorption, which is usually the main cause of laser damage to the crystal.[3] However, E_g is not the only factor influencing LIDT, laser radiation can also cause damage to the crystal due to thermal effects, which are closely related to local laser-induced heating in the crystal and the transfer of heating to the environment.[14] Thermal conductivity is a critical parameter in the design of high-power NLO devices, such as frequency doublers and optical parametric oscillators (OPOs). The nonlinear ambience should have sufficiently high thermal conductivity to ensure high LIDT and reduce the likelihood of thermolens formation,[5] and this will eventually increase the average output power.

A vivid example is the $LiGaS_2$ NLO crystal, which is characterized by the lowest SHG coefficient (d_{31} = 5.8 pm V^{-1}) in the

[a]*Sobolev Institute of Geology and Mineralogy SB RAS, Novosibirsk 630090, Russia. E-mail: lyudmila.isaenko@mail.ru*
[b]*Functional Crystals Lab, Technical Institute of Physics and Chemistry, Chinese Academy of Sciences, Beijing 100190, China. E-mail: zslin@mail.ipc.ac.cn*
[c]*Novosibirsk State University, Novosibirsk 630090, Russia*
[d]*Centre of Materials Science and Optoelectronics Engineering, University of Chinese Academy of Sciences, Beijing 100049, China*
[e]*Kutateladze Institute of Thermophysics SB RAS, Novosibirsk 630090, Russia*
†Electronic supplementary information (ESI) available. See DOI: https://doi.org/10.1039/d4qi02886d

This journal is © the Partner Organisations 2025

Inorg. Chem. Front., 2025, **12**, 1867–1873 | **1867**

ABC$_2$ family, but has the highest thermal conductivity (10 W m^{-1} K^{-1}), a significant band gap (4.15 eV) and the highest optical stability (with an LIDT of more than 240 MW per cm^2 vs. the values of 34 MW per cm^2 and 40 MW per cm^2 for AgGaS$_2$ and LiInS$_2$, respectively, at a pump of 1.064 nm and 15 ns).[15,16] Due to the combination of properties, the LiGaS$_2$ crystal exhibits good capability to obtain conversion efficiency in OPO systems that exceeds the performance of other representatives of this family. Also D. Chu and co-authors have developed a robust strategy for objective high-performance screening of more than 140 000 materials in order to study new NLO IR materials with high thermal conductivity and wide band gaps, which are crucial for determining the threshold of laser damage.[17] Thus, high thermal conductivity is of great practical importance for NLO crystals in the mid-IR range and is of increasing interest as one of the key indicators of material efficiency.

In semiconductors and insulators, where the IR NLO materials belong to, heat is mainly transferred by phonons,[18] i.e., the lattice thermal conductivity k_L determines the thermal conductivity. In a real crystal, the anharmonic oscillation frequencies of lattices change with changes in the mass of atoms,[19] their coordination in the lattice,[20] interatomic distances,[19] binding forces and emerging stresses. In general, an increase in the coordination of ions in the lattice leads to a decrease in k_L. Low thermal conductivity can also be caused by cationic or anionic vacancies, other points and extended defects.[21] However, the correlation between k_L and the structure in the IR NLO multicomponent chalcogenides is very complicated, and detailed research studies are still scarce. This is mainly because, on one hand, the experimental measures on k_L need large size chalcogenide crystals that are difficult to grow, and on the other hand, the theoretical studies, especially those based on first-principles, involve tedious phonon-relevant calculations that are very time-consuming. For instant and high-performance k_L research with low resource costs, an effective method is to adopt the machine learning (ML) method by using a well-trained algorithm based on existing k_L data and subsequently predicting k_L based on material structures directly. ML has been demonstrated to play an increasingly important role in high-performance screening of functional materials in many fields, including IR NLO chalcogenides.[19]

In this work the main attention is paid to the lattice thermal conductivity k_L of the solid solutions Li$_x$Ag$_{1-x}$Ga$_y$In$_{1-y}$Se$_2$ in ABC$_2$ chalcogenides. Totally, three cases of composition variations are considered: Li$_x$Ag$_{1-x}$BSe$_2$ (B = Ga and In) by varying the A-site cations and AgGa$_y$In$_{1-y}$Se2 by varying the B-site cations. Previous studies have shown that all these series have pretty strong SHG effects, wide IR transparency and relatively large energy band gaps.[8–12] Note that there are significant differences in the atomic mass and electronegativity of constituent atoms (Li, Ag, Ga, and In) in these series, which greatly affects the type and length of bonds between the atoms. Thus, the study of Li$_x$Ag$_{1-x}$BSe$_2$ (B = Ga and In) and AgGa$_y$In$_{1-y}$Se2 will allow us to evaluate the

changes in thermal conductivity when replacing heavy atoms Ag and In with light atoms Li and Ga. In addition, since in these series the tetragonal structure turns into an orthorhombic one with an increase in the lithium content,[8,9] it is possible to estimate the change in k_L with a change in the crystal structure. To investigate these issues, here we adopt the ML method with a well-trained TL-CGCNN algorithm which has been obtained based on the existing k_L data[19] to predict k_L directly from the material structures in the Li$_x$Ag$_{1-x}$Ga$_y$In$_{1-y}$Se$_2$ series. At the same time, an experimental laser flash method is used to measure the thermal conductivity of several materials in this series for confirmation. By combining ML data-mining with experimental measurements, the relationship between structural characteristics and k_L is analyzed, and some structural features that allow achieving a good balance among thermal and IR NLO performances in the multicomponent chalcogenides are obtained.

Results and discussion

Thermal conductivity in the Li$_x$Ag$_{1-x}$BSe$_2$ (B = Ga and In) and AgGa$_y$In$_{1-y}$se$_2$ series

The ML calculated data of the lattice thermal conductivity k_L for all three series of solid solutions Li$_x$Ag$_{1-x}$BSe$_2$ (B = Ga, In) and AgGa$_y$In$_{1-y}$Se$_2$ are presented in Fig. 1, as well as in Tables S2 and S3.† The structural symmetries of these compounds with respect to the variation of the A- and B-site cations are also shown in Tables S2, S3 and Fig. S1.† Compared to Table S1,† the predicted k_L data are consistent with the available experimental measurements. The ML calculation method
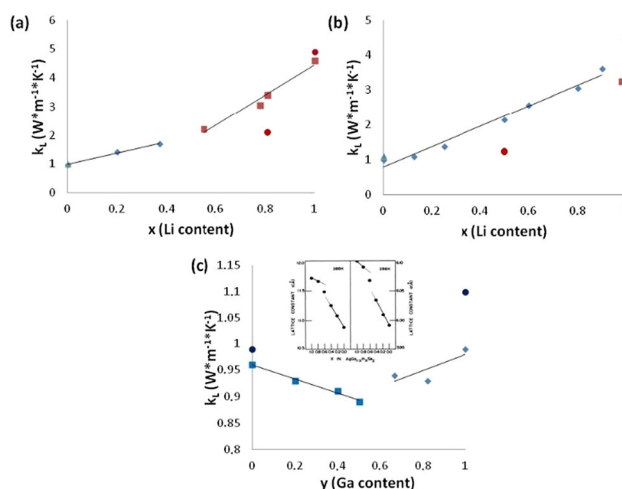

Fig. 1 The change in ML predicted thermal conductivity depending on the Li content for (a) Li$_x$Ag$_{1-x}$InSe$_2$ and (b) Li$_x$Ag$_{1-x}$GaSe$_2$, and on the Ga content for (c) AgGa$_y$In$_{1-y}$Se$_2$. The inset displays the change in the experimental cell parameters a and c from the In content for the solid solution AgGa$_y$In$_{1-y}$Se$_2$ in the previous study.[10] Solid lines are the least squares fittings of ML data and circles are experimental values. The solid solutions with a tetragonal symmetry ($I\bar{4}2d$) are indicated in blue, while those with a rhombic symmetry ($Pna2_1$) are indicated in red.

1868 | Inorg. Chem. Front., 2025, 12, 1867–1873

This journal is © the Partner Organisations 2025

is based on a graph neural network with CIF structural files as the only input information.[19] This means that the underlying mechanism cannot be directly interpreted from the model itself. However, the data obtained reflect a set of patterns linking k_L with the crystallographic features of the series of solid solutions $Li_xAg_{1-x}GaSe_2$, $Li_xAg_{1-x}InSe_2$, and $AgGa_yIn_{1-y}Se_2$. The crystallographic features we investigated include structural symmetry change, atomic mass, electronegativity difference, bond length, and atomic coordination number.

Structural symmetry change

In the $Li_xAg_{1-x}BSe_2$ (B = Ga, In) series, it is found that the lattice thermal conductivity of the compounds tends to increase as the Li/Ag ratio increases. Fig. 1a shows that the $k_L(x)$ dependence curve for the $Li_xAg_{1-x}InSe_2$ series can be represented by two straight lines with different inclination angles, which are determined by different structural symmetries $I\bar{4}2d$ and $Pna2_1$, respectively. This behavior of thermal conductivity reflects the structural changes in the system. These data are in good agreement with those obtained in ref. 9. Fig. 1b shows that the thermal conductivity of $Li_xAg_{1-x}GaSe_2$ also increases as the lithium content increases, but at $x = 0.98$ there are peculiarities on the curve with the decrease of k_L, and then increases at $x = 1$. This is also due to a change in the symmetry of the compounds. It is in this x range that the transition of $I\bar{4}2d$ to $Pna2_1$ has been experimentally recorded.[8] In the $AgGa_yIn_{1-y}Se_2$ series, the tetragonal space group remains unchanged throughout the range of $0 \leq y \leq 1$ (Table S3†). As shown in Fig. 1c, the dependence of k_L on the Ga/In ratio is somewhat complicated. The thermal conductivity in the $AgGa_yIn_{1-y}Se_2$ series decreases in the region $0 \leq y \leq 0.5$ with a decrease in the Ga content, and then increases in the region $0.7 \leq y \leq 1$. The inset in Fig. 1c displays the change in the experimental cell parameters a and c from the In content for the solid solution $AgGa_yIn_{1-y}Se_2$ in the previous study.[10] Based on the X-ray diffraction data, Hahn and Kim[10] pointed out that there are actually two regions of different tetragonal solutions with different positions of Ag and In, at y from 0 to 0.2 and at y from 0.6 to 1, respectively, in the $AgGa_yIn_{1-y}Se_2$ series. In the range $y = 0.4-0.5$, the dependence of the lattice constants undergoes a sharp change, the authors interpreted this region as the immiscibility region[10] (also see the inset in Fig. 1c). This region would be accompanied by a sharp decrease in k_L. Thus, the variation of thermal conductivity in Fig. 1c once again corresponds to the reorganization of the structures in $AgGa_yIn_{1-y}Se_2$.

Atomic mass

With an increase of the Li content (in Fig. S2a and S2b†) and the Ga content (in Fig. S2c†), the atomic mass (i.e., the molecular weight per formula unit) decreases (see Table S4†). This leads to an increase in thermal conductivity in the case of $Li_xAg_{1-x}InSe_2$ (Fig. 2a) and $Li_xAg_{1-x}GaSe_2$ (Fig. 2b), but a complex dependence on $AgGa_yIn_{1-y}Se_2$ (Fig. 2c) which shows the difference between these solid solutions.
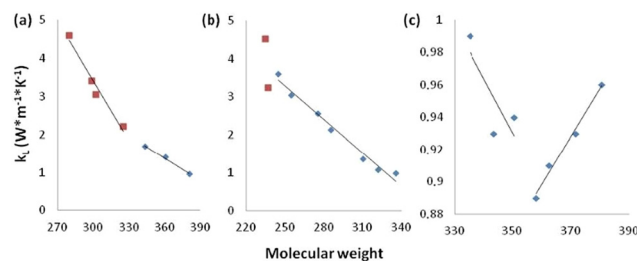

Fig. 2 The change in thermal conductivity depending on the molecular weight of (a) $Li_xAg_{1-x}InSe_2$, (b) $Li_xAg_{1-x}GaSe_2$ and (c) $AgGa_yIn_{1-y}Se_2$. Solid lines are the least squares fittings of ML data and circles are experimental values. The solid solutions with a tetragonal symmetry ($I\bar{4}2d$) are indicated in blue, while those with a rhombic symmetry ($Pna2_1$) are indicated in red.

Electronegativity difference

The lattice thermal conductivity increases with an increase in the electronegativity difference between cations and anions (Fig. 3 and Table S5†). Actually, the difference in electronegativity of atoms in a molecule determines the nature of the chemical bond: for a purely covalent one, the difference is zero, for a polar covalent one – 0.4–2.0 eV, for an ionic one – more than 2.0 eV.[22] In the $Li_xAg_{1-x}GaSe_2$ series, a polar covalent bond is observed at x from 0 to 0.6, but at x from 0.8 to 1 the ionic type of bond already prevails. In the $Li_xAg_{1-x}InSe_2$ system, the ionic bond is observed only in pure $LiInSe_2$. For the $AgGa_yIn_{1-y}Se_2$ series, electronegativity increases from 1.2 to 1.3 eV with an increase in the Ga content from 0 to 1 (Table S5†) and thus only the polar covalent bond between atoms is observed. However, owing to the initial decrease and subsequent increase in thermal conductivity for this series, the contribution of electronegativity is minimal.

Bond length

Thermal conductivity significantly depends on the bond length between atoms, with their increase it decreases in the
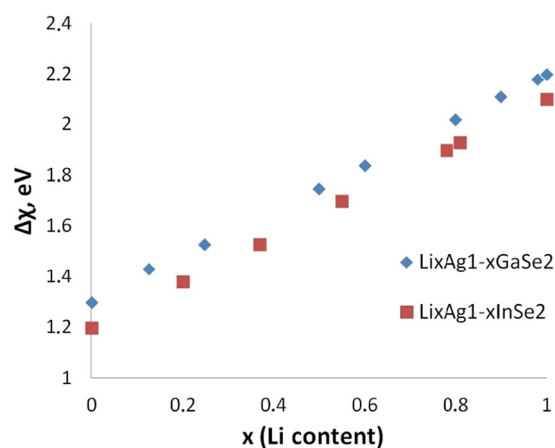

Fig. 3 The difference in electronegativity of $Li_xAg_{1-x}GaSe_2$ and $Li_xAg_{1-x}InSe_2$ systems.

This journal is © the Partner Organisations 2025

Inorg. Chem. Front., 2025, **12**, 1867–1873 | **1869**

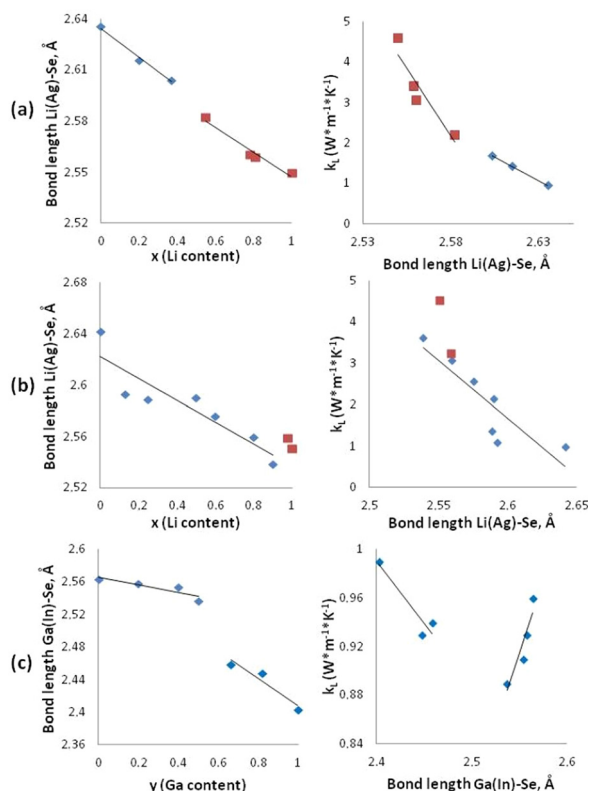**Fig. 4** The dependence of the Li(Ag)–Se bond length on the Li content and lattice thermal conductivity (k_L) in the structures of (a) $Li_xAg_{1-x}InSe_2$, (b) $Li_xAg_{1-x}GaSe_2$ and (c) $AgGa_yIn_{1-y}Se_2$.

$Li_xAg_{1-x}InSe_2$ system (Fig. 4a), the same dependence is also observed for $Li_xAg_{1-x}GaSe_2$ (Fig. 4b and Table S4†). In comparison, bond lengths Ga(In)–Se decrease differently for different tetragonal solid solutions $AgGa_yIn_{1-y}Se_2$ (Fig. 4c). The dependence of thermal conductivity k_L on molecular weight and bond lengths Ga(In)–Se are similar and show the difference between two tetragonal solid solutions of the series $AgGa_yIn_{1-y}Se_2$.

Atomic coordination number

Using the data obtained for these chalcogenide series in our articles[8,9] and other studies,[10–12] it is shown that all cations in these series have a coordination number equal to 4 in both tetragonal and orthorhombic phases, and the changing of the coordination number is not observed. Therefore, this factor will not affect the values of thermal conductivity in this case.

From all the above analysis on the thermal conductivity and structure relationship, one may reveal that in $Li_xAg_{1-x}InSe_2$ and $Li_xAg_{1-x}GaSe_2$, k_L is reduced with the increase in the atomic mass and length of Li(Ag)–Se bond as the Li content decreases from $x = 1$ to $x = 0$. Moreover, an increase in lattice thermal conductivity is observed with an increase in the electronegativity difference ($\Delta\chi$) between cations and anions, which is maximal at $x = 1$. When structural rearrangements appear in the system, the distortion of the lattice increases the

anharmonicity of lattice vibrations, which, along with the increased phonon scattering intensity due to the formation of defects, causes discontinuous changes in thermal conductivity near the phase transition. Additionally, it is important to understand which phonon frequencies are formed by the vibrations of one or both atoms in a complex compound. As shown in Fig. S3,† we studied the phonon spectra and phonon DOS of $LiGaSe_2$, $LiAgGa_2Se_4$, and $AgGaSe_2$. We found that the vibrations of the very light lithium atoms form the optical branch of the phonon spectrum. The contribution of the acoustic branch to thermal transfer is significant, as shown clearly in Fig. S3b and S3c.† This indicates that the increase in the content of Ag, with a high contribution to the acoustic branch, has a negative effect on the thermal conductivity.

In contrast to the $Li_xAg_{1-x}BSe_2$ (B = In, Ga) series, the non-monotonicity of thermal conductivity is presented in the $AgGa_yIn_{1-y}Se_2$ series. It is known that the strength of interatomic bonds strongly affects the thermal conductivity of a material. In ref. 12, a characteristic of the interatomic bond in the $AgInSe_2$ compound was given. It is shown that the interaction between Ag and Se is quite strong, while the interaction between the Ag–Se and in the cluster is rather weak. The authors[23] explained the low lattice thermal conductivity of $AgInSe_2$ by "cluster fluctuations" of Ag–Se at low phonon frequencies. These low-frequency optical phonons can provide additional channels of phonon scattering, which prevents the normal transport of acoustic phonons with close frequencies, and thus leads to low thermal conductivity.[24] When indium is replaced by gallium, the ratio of binding forces changes. At the same time, we observe a decrease in thermal conductivity in the $AgGa_yIn_{1-y}Se_2$ system with an increase in the light Ga content in the y range from 0 to 0.5. The obtained extraordinary result can also be explained by the anharmonicity of crystal lattice vibrations, and the scattering of phonons on the Ga_{In} defects which is significant when the Ga content is relatively low. In addition, experiments have observed the possibility of the formation of defects of Ga_{Ag} interatomic substitution and the concomitant formation of V_{Ag} silver vacancies in $AgGa_yIn_{1-y}Se_2$.[12] This is a widespread defect in chalcogenides, that also occurs in $LiGaS_2$ and $LiInSe_2$.[6,25] The effective ionic radius of Ga (0.47 Å) is significantly less than the effective ionic radius of silver (1.0 Å),[26] and the energy threshold for the formation of such an effect is very low.[24] In comparison, In_{Ag} defect is less likely to form, since the effective ionic radius of In (0.62 Å) is much larger than that of Ga. In this case, the decrease in lattice thermal conductivity can be partially explained by the scattering of phonons on the Ga_{In}, Ga_{Ag} and V_{Ag} defects. It can be assumed that the restructuring in the system ensures the formation of a more ordered structure at $y = 0.7$ after the immiscibility region, and the thermal conductivity increases as the content of light Ga in the solid solution increases and the total mass decreases at $y > 0.7$.

Balanced NLO performance

To search for effective materials used as NLO converters, the set of parameters to be optimized includes the band gap E_g,

1870 | *Inorg. Chem. Front.,* 2025, **12**, 1867–1873

This journal is © the Partner Organisations 2025

the nonlinear coefficient d_{ij}, birefringence (Δn) and optical stability. As a result of the above analysis, this list can be expanded to include thermal conductivity. The last parameter determines the efficiency of using crystals in laser systems.

For solid solutions $Li_xAg_{1-x}GaSe_2$ and $Li_xAg_{1-x}InSe_2$ an analysis that allows us to find the optimal combination of the thermal conductivity k_L values with the second harmonic generation coefficient and the band gap has been performed (Fig. 5 and Table S2†). For the $Li_xAg_{1-x}GaSe_2$ series the composition x = 0.8 can be selected, for which the maximum coefficient d_{ij} = 43 pm V^{-1} is observed, the band gap E_g = 2.22 eV and the thermal conductivity k_L = 3.06 W m^{-1} K^{-1}. For the $Li_xAg_{1-x}InSe_2$ series a significant increase in thermal conductivity occurs with an increase in the band gap. It is also possible to select the composition x = 0.81, for which the coefficient d_{ij} = 26.3 pm V^{-1}, the band gap E_g = 2.27 eV and the thermal conductivity k_L = 3.41 W m^{-1} K^{-1}. Fig. 5 highlights the areas, where k_L, d_{ij}, and E_g parameters are optimally combined for (a) $Li_xAg_{1-x}GaSe_2$ and (b) $Li_xAg_{1-x}InSe_2$.

Another important parameter for NLO materials is birefringence Δn. At values of Δn = 0.03–0.10 the conditions of phase synchronism are realized in a wide wavelength range.[6] However, to obtain such values a large anisotropy of the lattice is preferable, which in turn lowers the thermal conductivity due to the factor of increasing anharmonicity.[11] Fig. 5 shows the birefringence and thermal conductivity for $Li_xAg_{1-x}InSe_2$ and $Li_xAg_{1-x}GaSe_2$ systems.

We see that for the $Li_xAg_{1-x}GaSe_2$ system with a composition of x = 0.8, an optimal set of parameters k_L, d_{ij}, and E_g is observed, but birefringence turned out to be insufficient: $\Delta n <$ 0.01. To optimize this parameter, one needs to change the composition, reduce the lithium content x to 0.5 ($Li_{0.5}Ag_{0.5}GaSe_2$), then the combination of characteristics will be as follows: d_{ij} = 26 pm V^{-1}, E_g = 2.11 eV, k_L = 2.14 W m^{-1} K^{-1}, and Δn = 0.022. For the $Li_xAg_{1-x}InSe_2$ system the found optimum of the characteristics k_L, d_{ij}, and E_g with a composition x = 0.81 includes a completely satisfactory value Δn = 0.056 for a wide range of phase synchronism (from 2 to 13 microns).[6]

According to the calculations given in this work, in the $AgGa_yIn_{1-y}Se_2$ the composition $AgGa_{0.5}In_{0.5}Se_2$ has a thermal conductivity of 0.9 W m^{-1} K^{-1} and an SHG coefficient of d_{36} = 41 pm V^{-1}.[27] The combination of these properties is approximately the same as that of $AgGaSe_2$, indicating that $AgGa_{0.5}In_{0.5}Se_2$ would be an IR NLO material with balanced performance.

Computational and experimental methods

Theoretical calculations. All values of the lattice heat capacity k_L at 300 K are obtained by using an ML method with the TL-CGCNN algorithm, which offers instant and high-performance k_L research with a small expenditure of machine time. Our previous study determined reliable computational parameters for the TL-CGCNN algorithm in the convolutional neural network of the ML model, which were used for high-performance screening and pre-experimental design on the NLO chalcogenides with high thermal conductivity.[19] In this work, this well-trained TL-CGCNN method is directly adopted to predict and analyse the thermal conductivity of the $Li_xAg_{1-x}Ga_yIn_{1-y}Se_2$ series. On the other hand, density functional theory implemented in the CASTEP package[28] is used to calculate the SHG coefficients, energy band gaps and birefringence values in our studied multicomponent chalcogenides, and the computational details are presented in ref. 3.

Measurement of thermal conductivity. A non-stationary short-term heating method, *i.e.*, the laser flash method, is used to directly measure temperature conductivity k_T, a physical parameter that characterizes the rate of change (equalization) of the temperature of a substance in nonequilibrium thermal processes. Consequently, the thermal conductivity k of the studied material can be determined by taking into account the known values of the specific heat capacity C_p and density ρ, as well as k_T, using the formula $k = k_T \cdot C_p \cdot \rho$.[29]

Laser flash measurements at a given temperature T are carried out in a series of two laser "flashes" with an interval of 3 minutes after thermostating the sample on an automated LFA-427 device from NETZSCH (Germany) a high-purity argon atmosphere (99.992) in the temperature range 23–300 °C. The description of the measurement method and the experimental setup are presented in ref. 29 and 30. It is important to note that all samples had the same thickness since thickness is an important parameter for the laser "flash" method.
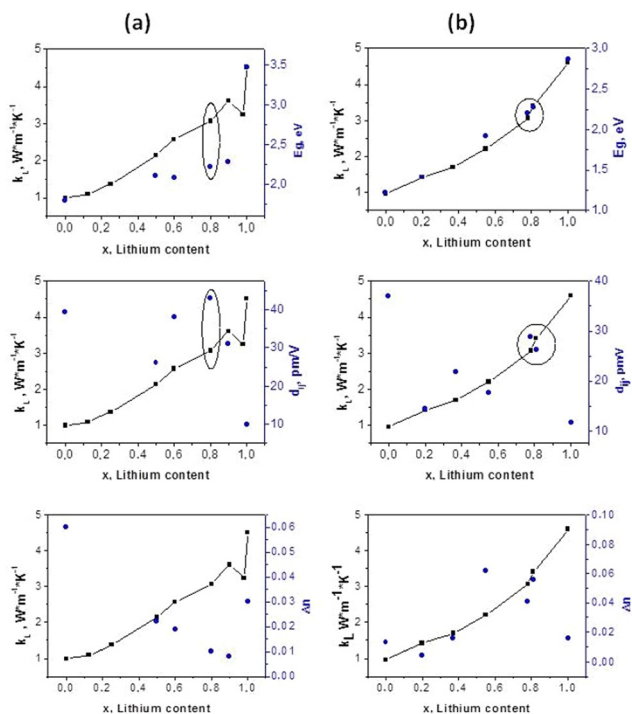

Fig. 5 The dependence of lattice thermal conductivity (k_L) and second harmonic generation (d_{ij}), band gap (E_g), birefringence (Δn) on the Li content for (a) the $Li_xAg_{1-x}GaSe_2$ system (left column) and (b) the $Li_xAg_{1-x}InSe_2$ system (right column).

This journal is © the Partner Organisations 2025

Inorg. Chem. Front., 2025, **12**, 1867–1873 | **1871**

Based on the laser flash method, we determine the thermal conductivity of LiInSe$_2$, LiGaSe$_2$, Li$_{0.8}$Ag$_{0.2}$InSe$_2$, Li$_{0.5}$Ag$_{0.5}$GaSe$_2$, AgGaSe$_2$, AgInSe$_2$ crystals. Table S1† shows the values of thermal conductivity, heat capacity and density of the listed crystals. In ref. 31, the experimental heat capacities of LiInS$_2$, LiInSe$_2$, LiGaS$_2$, LiGaSe$_2$ and LiGaTe$_2$ crystals in the temperature range of 180 to 460 K were obtained.[31] The thermal conductivity values of AgGaSe$_2$ and AgInSe$_2$ are taken from other sources.[32,33]

Conclusions

1. In this paper we present an effective approach to using TL-CGCNN machine learning programs to evaluate the thermal conductivity k_L of solid solutions: Li$_x$Ag$_{1-x}$BSe$_2$ (B = Ga and In) and AgGa$_y$In$_{1-y}$Se$_2$ with a smooth change in compositions x and y. The ML model with the TL-CGCN algorithm was used to predict the thermal conductivity of elementary compounds combined in symmetrical positions A and B of the ABC$_2$ system. The calculated data are in good agreement with the experiment.

2. In complex compounds it is important to understand which phonon frequencies are formed by vibrations of one or another atom of the compound. For example, LiGa(In)Se$_2$ vibrations of very light lithium atoms form the optical branch of the phonon spectrum. Optical phonons, as a rule, do not create significant thermal resistance in this compound. 100% replacement of lithium with heavy silver changes the picture—silver will participate in the formation of the acoustic branch of phonons along with Se and other heavy elements.

3. The found patterns of k_L dependence on mass, bond length between atoms, and electronegativity of atoms allow us to navigate in the process of searching for new chalcogenide crystals with an optimal set of parameters that allow them to be effectively used as a frequency converter of laser radiation in the IR range.

4. In two systems of solid solutions Li$_x$Ag$_{1-x}$InSe$_2$ and Li$_x$Ag$_{1-x}$GaSe$_2$, the compositions Li$_{0.5}$Ag$_{0.5}$GaSe$_2$ and Li$_{0.81}$Ag$_{0.19}$InSe$_2$ were found to provide a balanced combination of the parameters k_L, d_{ij}, E_g, and Δn. A sufficiently high value of their thermal conductivity provided high optical stability: 1 GW and 0.4 GW for Li$_{0.5}$Ag$_{0.5}$GaSe$_2$ and Li$_{0.81}$Ag$_{0.19}$InSe$_2$, respectively (τ = 0.5 ns and λ = 1.064 μm).[34,35] In AgGa$_y$In$_{1-y}$Se$_2$, AgGa$_{0.5}$In$_{0.5}$Se$_2$ is predicted to be an IR NLO material with balanced performance.

The results of this work demonstrate not only an effective strategy, but also determine research directions in the search for crystals with balanced NLO characteristics in the mid-IR range, including high thermal conductivity, which plays a crucial role in LIDT enhancement in IR NLO crystals.

Data availability

Data are available on request from the authors.

Conflicts of interest

There are no conflicts to declare.

Acknowledgements

References

1 H. Chen, M.-Y. Ran, W.-B. Wei, X.-T. Wu, H. Lin and Q.-L. Zhu, A comprehensive review on metal chalcogenides with three-dimensional frameworks for infrared nonlinear optical applications, *Coord. Chem. Rev.*, 2022, **470**, 214706.

2 P. Gong, F. Liang, L. Kang, X. Chen, J. Qin, Y. Wu and Z. Lin, Recent advances and future perspectives on infrared nonlinear optical metal halides, *Coord. Chem. Rev.*, 2019, **380**, 83–102.

3 Z. Lin, X. Jiang, L. Kang, P. Gong, S. Luo and M.-H. Lee, First-principles materials applications and design of nonlinear optical crystals, *J. Phys. D: Appl. Phys.*, 2014, **47**, 253001.

4 A. A. Manenkov, Fundamental mechanisms of laser-induced damage in optical materials: today's state of understanding and problems, *Opt. Eng.*, 2014, **53**, 010901.

5 S. G. Sabouri, S. C. Kumar, A. Khorsandi and M. Ebrahim-Zadeh, Thermal Effects in High-Power Continuous-Wave Single-Pass Second Harmonic Generation, *IEEE J. Sel. Top. Quantum Electron.*, 2014, **20**, 563–572.

6 L. I. Isaenko and A. P. Yelisseyev, Recent studies of nonlinear chalcogenide crystals for the mid-IR, Semicond, *Sci. Technol.*, 2016, **31**, 123001.

7 J. Huang, S. Shu and G.-M. Cai, Screening Nitrides with High Debye Temperatures as Nonlinear Optical Materials, *J. Phys. Chem. C*, 2022, **126**, 7047–7053.

8 L. Isaenko, L. Dong, A. Kurus, Z. Lin, A. Yelisseyev, S. Lobanov, M. Molokeev, K. Korzhneva and A. Goloshumova, Li$_x$Ag$_{1-x}$GaSe$_2$: Interplay Between Lithium and Silver in Mid-Infrared Nonlinear Optical Chalcogenides, *Adv. Opt. Mater.*, 2022, **10**, 2201727.

9 L. Isaenko, L. Dong, K. Korzhneva, A. Yelisseyev, S. Lobanov, S. Gromilov, M. S. Molokeev, A. Kurus and Z. Lin, Evolution of Structures and Optical Properties in a Series of Infrared Nonlinear Optical Crystals Li$_x$Ag$_{1-x}$InSe$_2$ (0 ≤ x ≤ 1), *Inorg. Chem.*, 2023, **62**, 15936–15942.

10 S.-R. Hahn and W.-T. Kim, Anomalous composition and temperature dependence of the energy gap of AgGa$_{1-x}$In$_x$Se$_2$ mixed crystals, *Phys. Rev. B: Condens. Matter Mater. Phys.*, 1983, **27**, 5129–5131.

11 J. E. Avon, K. Yoodee and J. C. Woolley, Solid solution, lattice parameter values, and effects of electronegativity in the $(Cu_{1-x}Ag_x)(Ga_{1-y}In_y)(Se_{1-z}Te_z)_2$ alloys, *J. Appl. Phys.*, 1984, **55**, 524–535.

12 V. V. Badikov, G. M. Kuz'micheva, V. L. Panyutin, V. B. Rybakov, V. I. Chizhikov, G. S. Shevyrdyaeva and S. I. Shcherbakov, Preparation and Structure of $AgGa_{1-x}In_xSe_2$ Single Crystals, *Inorg. Mater.*, 2003, **39**, 1028–1034.

13 L. Isaenko, I. Vasileva, A. Yelisseyev, P. Krinitsin and S. Lobanov, Recent studies of nonlinear chalcogenide crystals for the mid-IR. The 16th, *Int. Conf. on Crystal Growth*, Book of Abstracts (Beijing: ICCGE), 2010, p. 10.

14 M. Currie, J. D. Caldwell, F. J. Bezares, J. Robinson, T. Anderson, H. Chun and M. Tadjer, Quantifying pulsed laser induced damage to graphene, *Appl. Phys. Lett.*, 2011, **99**, 211909.

15 D. N. Nikogosyan, *Nonlinear Optical Crystals: A Complete Survey*, 2005.

16 V. Petrov, Progress in 1-μm Pumped Mid-IR Optical Parametric Oscillators Based on Non-Oxide Nonlinear Crystals, *IEEE J. Sel. Top. Quantum Electron.*, 2015, **21**, 193–206.

17 D. Chu, Y. Huang, C. Xie, E. Tikhonov, I. Kruglov, G. Li, S. Pan and Zh. Yang, Unbiased screening of novel infrared nonlinear optical materials with high thermal conductivity: long-neglected Nitrides and popular chalcogenides, *Angew. Chem.*, 2023, **135**, e202300581.

18 A. V. Inyushkin, Thermal conductivity of group IV elemental semiconductors, *J. Appl. Phys.*, 2023, **134**, 221102.

19 Q. Wu, L. Kang and Z. Lin, A Machine Learning Study on High Thermal Conductivity Assisted to Discover Chalcogenides with Balanced Infrared Nonlinear Optical Performance, *Adv. Mater.*, 2024, **36**, 2309675.

20 D. P. Spitzer, Lattice thermal conductivity of semiconductors: A chemical bond approach, *J. Phys. Chem. Solids*, 1970, **31**, 19–40.

21 P. Qiu, Y. Qin, Q. Zhang, R. Li, J. Yang, Q. Song, Y. Tang, S. Bai, X. Shi and L. Chen, Intrinsically High Thermoelectric Performance in $AgInSe_2$ n-Type Diamond-Like Compounds, *Adv. Sci.*, 2018, **5**, 1700727.

22 S. S. Batsanov, *Structural chemistry*, Dialog-Moscow State University, Moscow, 2000.

23 Y. Zhu, B. Wei, J. Liu, N. Z. Koocher, Y. Li, L. Hu, W. He, G. Deng, W. Xu, X. Wang, J. M. Rondinelli, L.-D. Zhao, G. J. Snyder and J. Hong, Physical insights on the low lattice thermal conductivity of $AgInSe_2$, *Mater. Today Phys.*, 2021, **19**, 100428.

24 S. Ozaki and S. Adachi, Temperature dependence of the lowest-direct-bandgap energy in the ternary chalcopyrite semiconductor $AgInSe_2$, *J. Mater. Sci.:Mater. Electron.*, 2007, **18**, 25–28.

25 Y. Li, X. Zhao and X.-f. Cheng, Point Defects and Defect-Induced Optical Response in Ternary $LiInSe_2$ Crystals: First-Principles Insight, *J. Phys. Chem. C*, 2015, **119**, 29123–29131.

26 R. D. Shannon, Revised effective ionic radii and systematic studies of interatomic distances in halides and chalcogenides, *Acta Crystallogr., Sect. A*, 1976, **32**, 751–767.

27 M. A. Yu, I. S. Baturin, P. P. Geiko and A. I. Gusamov, CO_2 laser frequency doubling in a new nonlinear $AgGa_xIn_{1-x}Se_2$ crystal, *Quantum Electron.*, 1999, **29**, 904.

28 S. J. Clark, M. D. Segall, C. J. Pickard, P. J. Hasnip, M. I. J. Probert, K. Refson and M. C. Payne, First principles methods using CASTEP, *Z. Kristallogr. – New Cryst. Struct.*, 2005, **220**, 567–570.

29 W. J. Parker, R. J. Jenkins, C. P. Butler and G. L. Abbott, Flash Method of Determining Thermal Diffusivity, Heat Capacity, and Thermal Conductivity, *J. Appl. Phys.*, 1961, **32**, 1679–1684.

30 I. V. Savchenko and S. V. Stankus, Thermal conductivity and thermal diffusivity of tantalum in the temperature range from 293 to 1800 K, *Thermophys. Aeromech.*, 2008, **15**, 679–682.

31 V. A. Drebushchak, L. I. Isaenko, S. I. Lobanov, P. G. Krinitsin and S. A. Grazhdannikov, Experimental heat capacity of $LiInS_2$, $LiInSe_2$, $LiGaS_2$, $LiGaSe_2$, and $LiGaTe_2$ from 180 to 460 K, *J. Therm. Anal. Calorim.*, 2017, **129**, 103–108.

32 H. J. Hou, F. J. Kong, J. W. Yang, L. H. Xie and S. X. Yang, First-principles study of the structural, optical and thermal properties of $AgGaSe_2$, *Phys. Scr.*, 2014, **89**, 065703.

33 H. Neumann, J. Łażewski, P. T. Jochym and K. Parlinski, Ab initio heat capacity and atomic temperature factors of chalcopyrites, *Phys. Rev. B: Condens. Matter Mater. Phys.*, 2007, **75**, 224301.

34 A. Yelisseyev, S. Lobanov, M. Molokeev, S. Zhang, A. Pugachev, Z. Lin, V. Vedenyapin, A. Kurus, A. Khamoyam and L. Isaenko, A New Nonlinear Optical Selenide Crystal $AgLiGa_2Se_4$ with Good Comprehensive Performance in Mid-Infrared Region, *Adv. Opt. Mater.*, 2021, **9**, 2001856.

35 L. Isaenko, L. Dong, A. Yelisseyev, S. Lobanov, K. Korzhneva, S. Gromilov, A. Sukhih, A. Pugachev, V. Vedenyapin, A. Kurus, A. Khamoyan and Z. Lin, A new nonlinear optical crystal $Li_{0.81}Ag_{0.19}InSe_2$ with balanced properties for efficient nonlinear conversion in the mid-IR region, *J. Alloys Compd.*, 2023, **969**, 172382.